

# MURPHY'S LAW AND THE PILE PREDICTION EVENT AT THE 2002 ASCE GEOINSTITUTE'S DEEP FOUNDATIONS CONFERENCE

Bengt H. Fellenius, Moh Hussein, Paul Mayne, and Ross T. McGillivray



Photo courtesy of Wayne Waters, PDCA

Fellenius, B.H., Hussein, M., Mayne, P., and McGillivray, R.T., 2004. Murphy's Law and the Pile Prediction Event at the 2002 ASCE GeoInstitute's Deep Foundations Conference, Deep Foundations Institute Meeting on Current Practice and Future Trends in Deep Foundations, Vancouver, September 29 - October 1, pp. 29 - 43.

# Murphy's Law and the Pile Prediction Event at the 2002 ASCE Geolnstitute's Deep Foundations Conference

Bengt H. Fellenius<sup>1)</sup>, Moh Hussein<sup>2)</sup>, Paul Mayne<sup>3)</sup>, and Ross T. McGillivray<sup>4)</sup>

<sup>1)</sup> Bengt Fellenius Consultants Inc, 1905 Alexander Street SE, Calgary, AB, T2G 4J3. <Bengt@Fellenius.net>

<sup>2)</sup> GRL Engineers Inc., 8008 South Orange Avenue, Orlando, FL, 32809. <MHGRLFL@aol.com>

<sup>3)</sup> Georgia Inst. of Technology, Civil Engng, 790 Atlantic Drive, Atlanta, GA 30332-0355. <Paul.Mayne@ce.gatech.edu>

<sup>4)</sup> Ardaman & Associates, Inc., 3925 Coconut Palm Drive, Suite 115, Tampa, FL, 33619. <RMcGillivray@ardaman.com>

**ABSTRACT:** The "Pile Prediction Event" at the ASCE Geolnstitute's Deep Foundation Conference in February 2002 involved prediction of drivability and capacity of three 14m long, 324mm diameter, closed-toe pipe piles driven into loose to compact fine sand to slightly silty sand. Predictors were provided the results of two soil borings and three cone penetrometer tests, as well as type and model of hammer to be used for the pile driving. A total of 33 persons submitted predictions. As to penetration resistance distribution, many predictions were far below actually observed values. As to capacity in compression, the predicted values ranged from 270KN through 2,340KN with a mean of 1,070KN. As to capacity in tension, the predicted values ranged from 100KN through 1,650KN. The maximum load applied to the compression pile in the static loading test was 1,250KN, at which no more reaction load was available. The reaction system for the tension test failed early in the test. CAPWAP analysis on End-of-Driving blows showed capacities at the end of the driving for the push and pull piles of 670KN, and 710KN, respectively. No restrrike tests were made. Additional CPT soundings indicate that the pile driving had densified the soil. Static analysis and calculations from the CPT indicated that capacities ranged from 1,000KN through 2,000KN. The paper presents the data and discusses the various methods of determining pile capacity and addresses influence of set-up. Lessons useful for future similar events are indicated.

## INTRODUCTION

A "Pile Prediction Event" was sponsored by the Pile Driving Contractors Association, PDCA, at the ASCE Geolnstitute's Deep Foundation Conference in February 2002. The event was part of an afternoon outing at the conference and involved three closed-toe pipe piles located about 15 m apart. The pile diameter was 324 mm (12.75 inch) and each pile was driven to 14.0 m embedment depth. Two of the piles, which had been driven well before the conference (on November 26, 2001) were subjected to static loading tests in compression (push test) and tension (pull test) on February 15, 2002. That same day, the third pile was driven as a pile driving demonstration (demo pile). Well before the conference, participants were invited to predict how the push and pull piles would behave in the static loading tests and what the penetration resistance (blow count) would be for the demo pile. The predictors were provided detailed information on pile size and length, soil profile, and driving equipment and driving procedure. A summary of the event was published by Goble (2002). Though the event also demonstrated the truth of Murphy's Law, (i.e. "what can go wrong, will go wrong"), the following detailed compilation of the results should be of more than passing interest to geotechnical engineers and deep foundation contractors. It may also be useful as a guide to how to avoid or minimize the impact of Murphy's Law in future similar events.

## SOIL PROFILE

The predictors were supplied with the results of two borings with SPT data and three piezocone soundings obtained in September 2001. The SPT N-indices are presented in Fig. 1. Dynamic monitoring established that the impact energy transferred to the SPT rods was close to the  $N_{60}$ -value. The pile embedment depth is indicated in the solid bar to the right of the diagram. The open bar immediately below the pile toe has a length of 4 pile diameter and represents the soil zone below the pile that most influences the pile toe capacity (the length of this zone is usually considered to range from 4 to 6 pile diameters).

The area is flat and the groundwater table at the site lies at a depth of 1.7 m, as established from CPTU soundings on September 21, 2001, and March 1, 2002. The soil profile was described to be composed of fine sand to slightly silty sand, though, in BH-1, a 0.2 m thick layer of gray clay was identified at a depth of 12.3 m. The two N-index profiles (Fig. 1) are very similar and indicate that the sand is loose to about 2.5 m depth, and then compact to 5 m depth.

The sand underlying these strata is loose to about 14 m depth. N-index at Depth 15 m in BH-2 was 28 bl/0.3m, which is representative of dense sand, and BH-1 indicated 4 bl/0.3m, representative of loose sand.

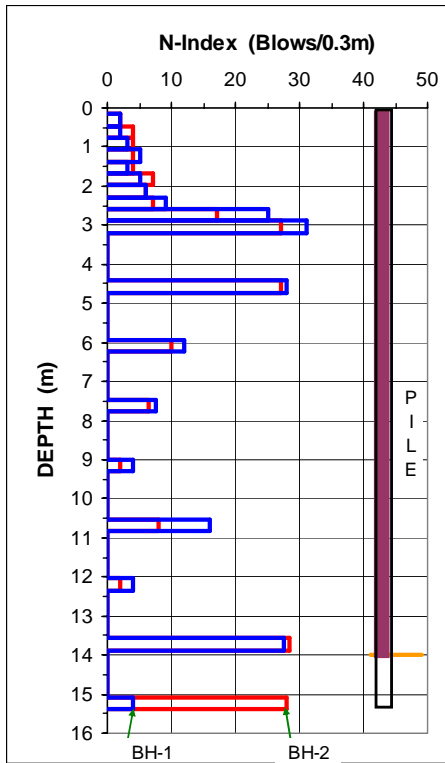


Fig. 1 Profile of SPT N-indices provided to predictors

Fig. 2A and 2B present the results of the three piezocone soundings made available to the predictors. CPT-1 and CPT-2 recorded the pore pressures at the U1 position, and CPT-M (Fig. 2A) recorded pore pressure at the U2 position. Soundings CPT-1 and CPT-2 were terminated in the sand at depths of 15.4 m and 15.5 m, respectively, while CPT-M was terminated at a depth of 18.6 m. Profiling using the CPT results indicates that the soil deposit is mostly sand with layers of fine sand and silty sand. The CPT-M indicates a 0.3 m thick layer of soft silty clay at 12.4 m depth, agreeing with the soil sample from BH-1 at the same depth, and shows that the sand is deposited on a clay layer at 16.0 m depth, just about 6 pile diameters below the pile toe.

When considering the response of a pile to loading, the soil conditions within a zone extending about 4 to 6 diameters below the pile toe govern pile toe load-movement (Eslami and Fellenius 2002). The three CPTU soundings indicate different soil types within this zone as shown in Fig. 3 presenting a zoomed-in diagram of the soil layers near the pile toe. The interpretation of the soil types according to the Eslami-Fellenius method (Eslami 1996; Eslami and Fellenius 2002) is that the soils consist of clean sand in this zone. For CPT-2, the sand includes layers or lenses of clay and silt.

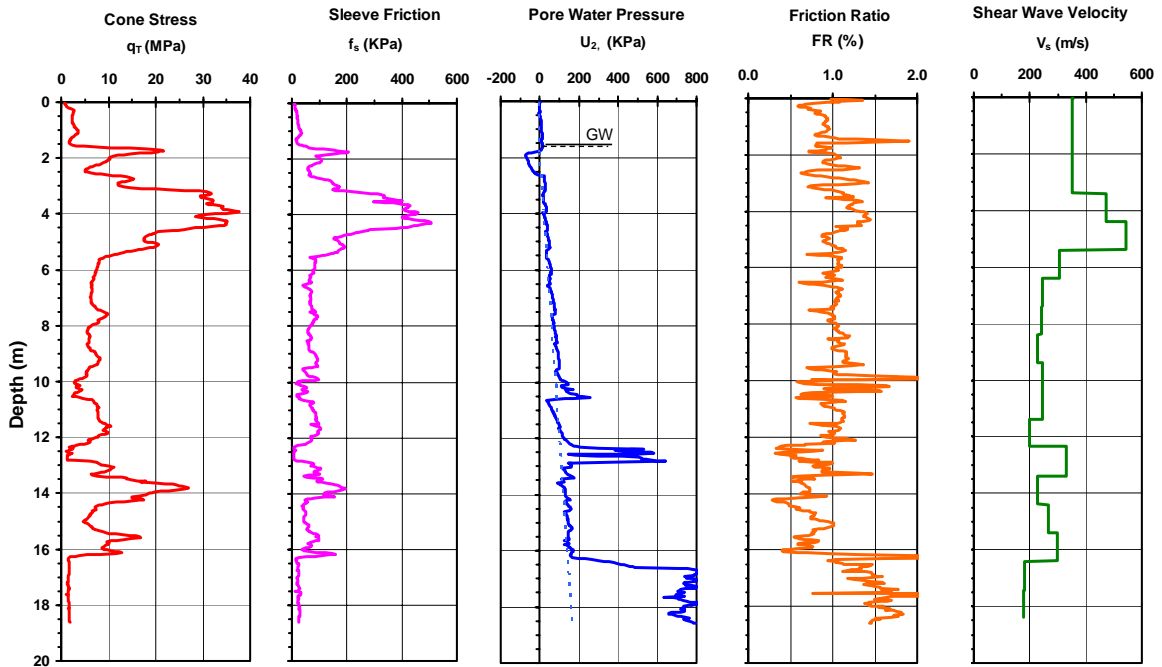


Fig. 2A Profile of CPT-M provided to predictors with shear wave measurements

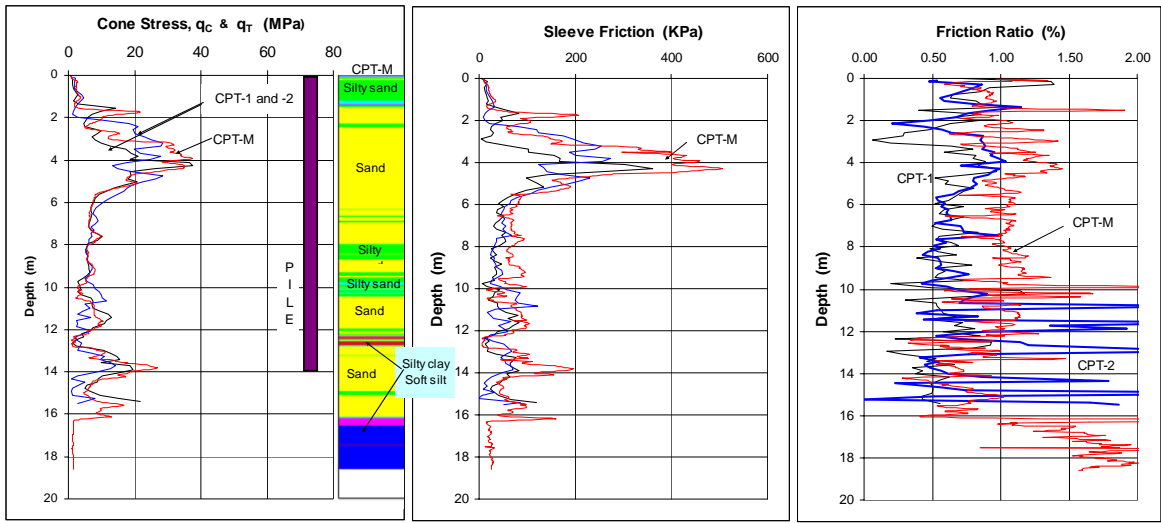


Fig. 2B Compiled profiles of cone penetrometer tests, CPT-1, CPT-2, and CPT-M supplied to predictors

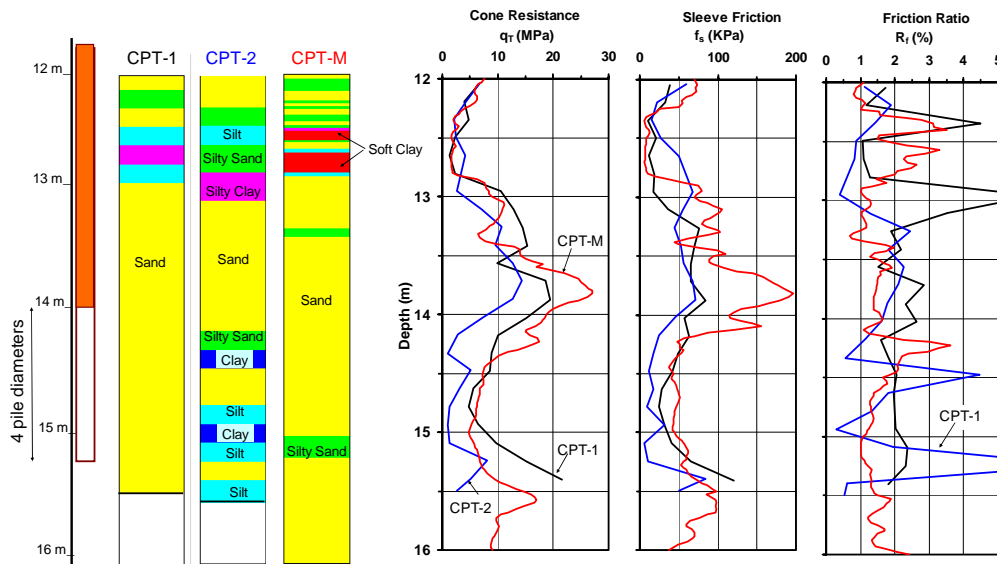


Fig. 3 CPT results for the depth range that governs pile toe resistance

The lay-out of the boreholes, CPTU soundings, and piles is presented in Fig. 4. The soil borings and CPTU soundings were put down about 80 m apart and about 40 m and 70 m away from where the three test piles were later driven. On March 1, 2002, two weeks after the conference, in order to more closely check out the soil profile at the test site, three additional CPTU soundings, CPT-3, CPT-4, and CPT-5, were made: CPT-3 was located 1.5 m east of the demo pile, CPT-4 at 7 m east of the pull pile and 7 m west of the push pile, and CPT-5 at 3 m east of the push pile. The results of the new soundings are

presented in Fig. 5 and indicate a soil type profile very similar to that indicated in the before-the-event soundings, except that the sand contains fewer layer of fines. The soft layer noticed in the first soundings at 12.3 m exists also at the test site. A thin clay layer is indicated in CPT-3 just below the pile toe, but, generally, the soil within 2 m (6 pile diameters) below the pile toe consists of sand, and the three soundings show similar values of cone stress, sleeve friction, and friction ratio in a narrow band slightly below the pile toe depth. This area near the pile toe is detailed in the zoomed-in cone stress diagrams shown in Fig. 6.

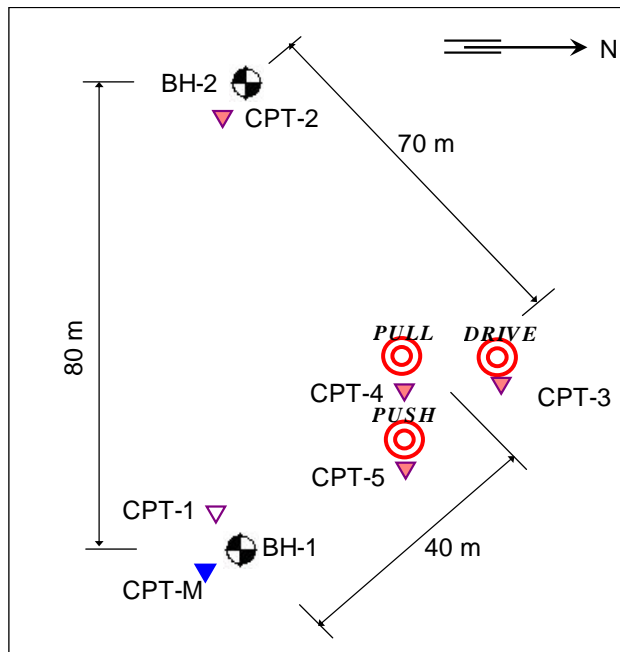


Fig. 4 Plan view over the locations of boring, CPT soundings, and piles

The largest difference between the previous and the new soundings is that in a zone between depths of about 4.0 m and 5.0 m, the soil is very much denser for the new soundings. Fig. 7 presents a comparison between the before-the-event soundings and the after-the-event soundings, showing a compilation of cone stress and sleeve friction curves. The figure demonstrates that both cone stress and sleeve friction for the after-the-event soundings are much larger in the dense, shallow layer as opposed to the values in the before-the-event soundings. This could either indicate that the dense, shallow sand layer is “naturally” denser or that the pile driving has densified the sand in this layer. Note that in comparison, the difference between the two sets of soundings is insignificant in the soil layer below the dense, shallow layer.

#### USE OF THE SOIL DATA FOR PREDICTION OF CAPACITY

In general, N-indices with classification of soil samples in combination with observations made during the field work (recovery ratio, water discharge, etc.) and the overall geology of the site provide the experienced soils engineer with important information that is helpful in assessing site conditions and, eventually, establishing foundation design recommendations. However, separating the N-indices from that experience and overall field work information and using the numerical values as “stand-alone” input to formulae or used in computer

processing should be considered highly unreliable (e.g., CFEM 1992). Numerical formulae based on N-indices are yet in common use. For example, Meyerhof (1976) suggested that the shaft and toe resistances can be calculated as indicated in Eqs. 1 and 2.

$$(1) \quad R_s = 400 N D A_s$$

$$(2) \quad R_t = 2 N A_t$$

$R_s$  = shaft resistance (KN)

$R_t$  = toe resistance (KN)

$N$  = N-index (bl/0.3m)

$D$  = embedment depth or length for which the N-index applies

$A_s$  = pile unit circumferential area (m<sup>2</sup>/m)

$A_t$  = pile toe area (m<sup>2</sup>)

Input of the N-indices from the two boreholes into the two Meyerhof formulae (directly for shaft resistance and the average N-index over the applicable depths of 11.0 m through 15.5 m for toe resistance), results in shaft resistance of 390 KN, same for both borings, and a toe resistance ranging from 400 KN to 530 KN. The calculated total pile capacities are 790 KN and 940 KN.

Several methods exist for calculating pile capacity from CPT and CPTU sounding results (e.g., Eslami 1996, Fellenius and Eslami 1997). Five methods were applied to the six soundings and the results are presented in Fig. 8. The top diagram shows the calculated capacity and the two lower diagrams show the calculated shaft and toe resistances, respectively, for the six soundings and the five methods. For comparison, the values derived from the SPT N-indices were added and a line was drawn to indicate the maximum test load that was applied to the compression pile in the static loading test. The results show a spread between methods and soundings with the results from using CPT-2 being the lowest. The results from CPT-5, the sounding closest to the pile that actually was subjected to a static loading test, are plotted with a line heavier than those of the others. The calculation results are compiled in Table 1.

Results of applying the methods to calculate the distribution of resistance (load distribution) in the soil along the pile are presented in Fig. 9. The slopes of the distribution curves are quite similar, which indicates a similar shaft resistance, except within a zone between about 4 m and about 5 m depth, where the indicated shaft resistance is much larger for the after-the-event soundings.

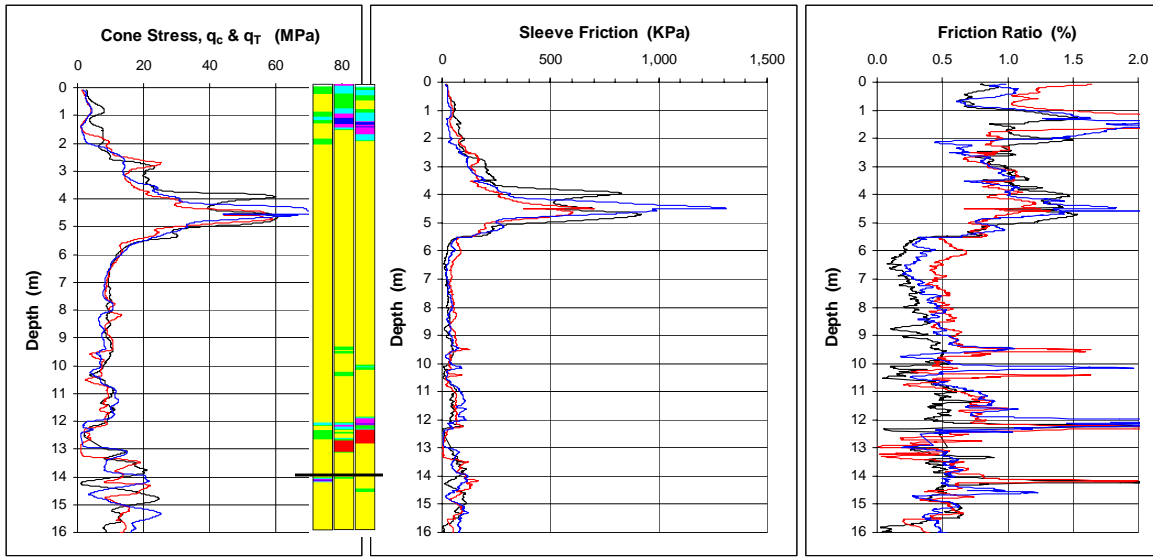


Fig. 5 Cone penetrometer soundings CPT-3, CPT-4, and CPT-5 near the piles obtained after the event

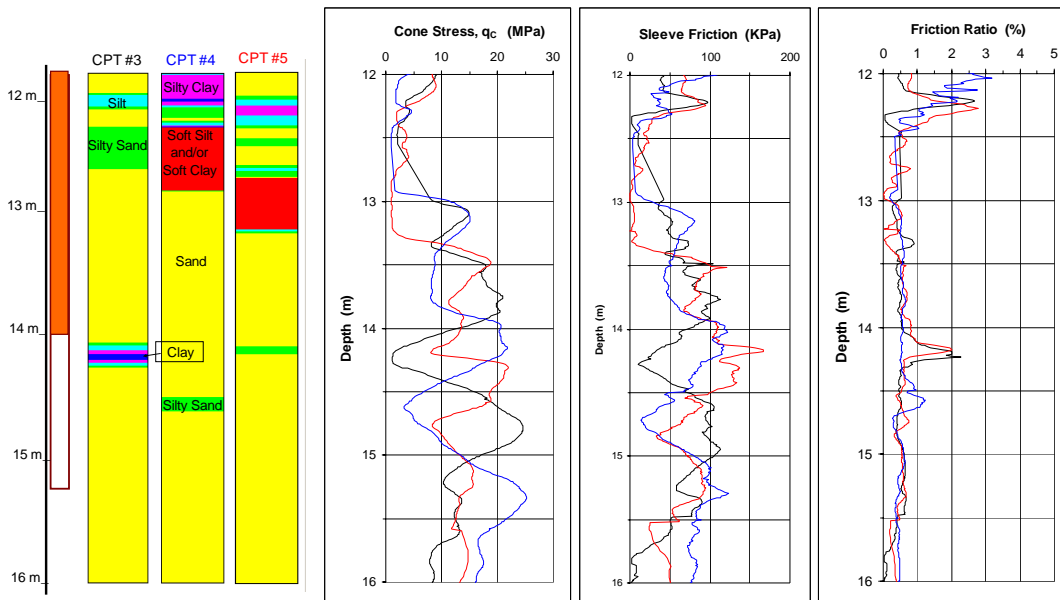


Fig. 6 CPT results at the pile site for the depth range that governs pile toe resistance

**Table 1 Capacities from five CPT methods applied to CPT-5**

Method:	Eslami Fellenius	Dutch	LCPC	Meyerhof	Schmertmann
Capacity (KN):	1,600	995	1,220	1,915	1,110

CPT-1 and CPT-2

Original CPTU soundings provided to the predictors  
The distance away from the pile site is 40m and 70m

CPT-3 — CPT-5

New CPTU soundings at the location of the test piles

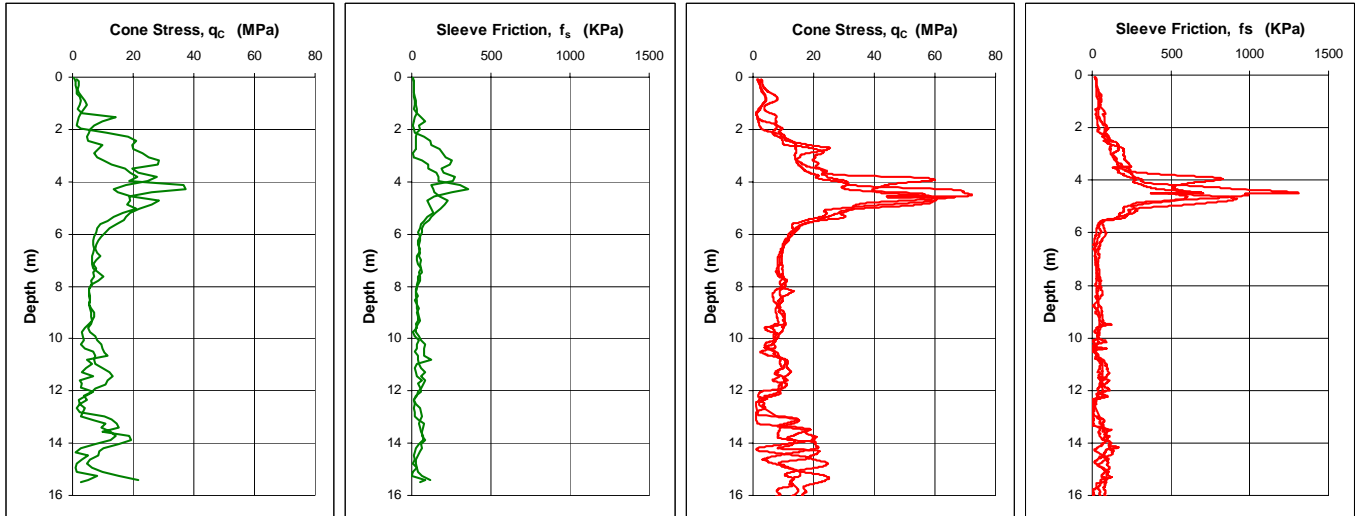


Fig. 7 Comparison between the CPTs provided to predictors and the CPTs obtained after the event

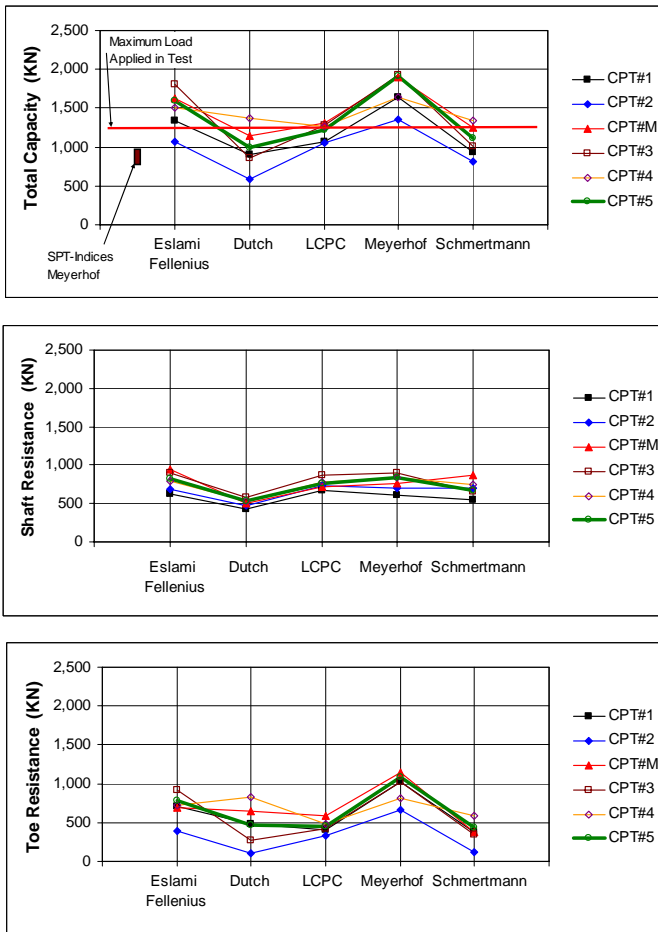


Fig. 8 Capacity from five CPTU methods for the six CPTUs  
Calculations performed with the UniCone program  
(Fellenius and Infante 2002)

It is enlightening to match the results of the CPT calculations to analysis of the pile resistance distribution using effective stress analysis. Fig. 10 presents a match for CPT-M. The two curves in the middle show the resistance distribution determined for CPT-M matched to a curve that applies the beta-coefficients indicated to the left in the diagram. Two additional resistance distribution curves are included for reference (shown with frequent small dots on the curve). The curve to the left applies a beta-coefficient equal to 0.5 throughout and a toe bearing coefficient equal to 40. Both values are usually considered representative of compact to dense sand. The curve to the right applies a beta-coefficient of 1.0 and a toe bearing coefficient of 60. The latter values are higher than usually considered applicable in sand and the curve is intended to be representative of an upper boundary. For reference to the prediction site, a beta-coefficient of 1.0 can be back-calculated from an O-cell test on a precast prestressed pile driven at Vilano Beach not too far from the Orlando demonstration site (McVay et al. 1999). The toe coefficient of 60 is selected as being reasonable for a beta-coefficient equal to 1.0. Indeed, the 3.8-beta value necessary to achieve the match to the CPT-M results in the very dense zone between the depths of 4 m and 5 m is unusually large. Moreover, the toe-bearing coefficient of 65 does not agree very well with a beta-coefficient of 0.3. Obviously, the results of the analysis of the CPT soundings indicate that the soil conditions at the site are unusual.

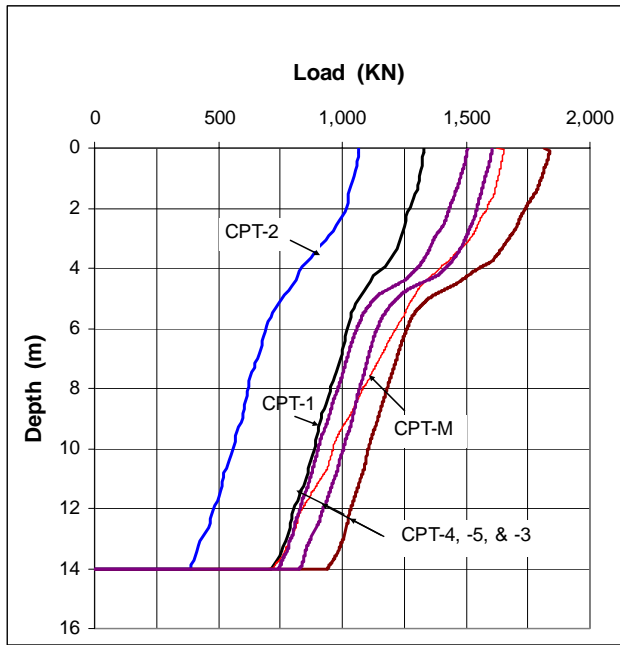


Fig. 9 Distribution of ultimate resistance from CPTU results according to the Fellenius Eslami-method. Calculations are performed with the UniCone program (Fellenius and Infante 2002)

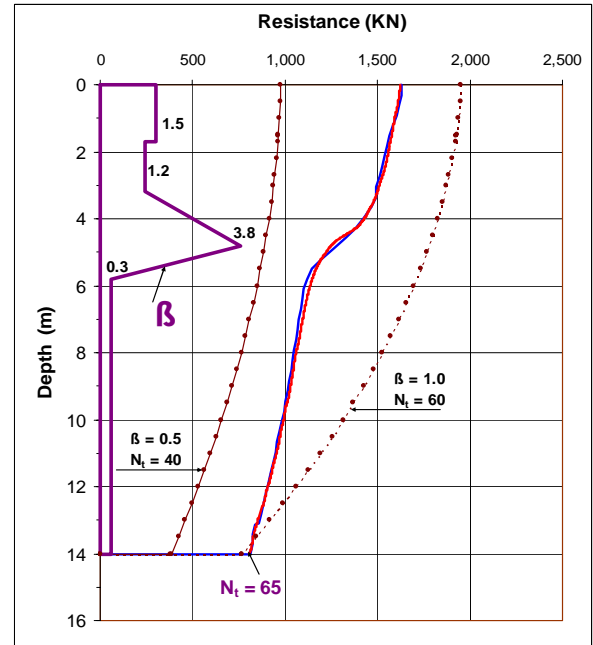


Fig. 10 Distribution of ultimate resistance from results of analysis matching the CPT-M sounding to effective stress and compared to upper and lower range of effective stress parameters. Calculations performed with the UniPile program (Fellenius and Goudreault 1998)

## THE PREDICTIONS OF CAPACITY

The foregoing represents all the information available to the predictors plus the results of CPT-3, CPT-4, and CPT-5 soundings made after the event. Because of the differences between the individual borings and soundings, as well as between the original information and that from the actual test site, it is obvious that all predictions, in the final analysis, must be tempered with a good measure of judgment.

A compilation of the predicted capacity for the push and pull pile is presented in Fig. 11. Two predictors submitted values of 5,295 KN (1,332 kips) and 6,380 KN (1,436 kips) which are very much higher than the others. Presumably, the predictors confused SI-units (KN) and English units (kips), intending to indicate kips, but wrote KN. As it is not possible to learn the truth and in order to maintain a reasonable scale, these two values have been excluded from Fig. 11.

It is presumed that the predictors would have stated (had they been asked) that the pull pile predicted capacity value is representative of the shaft

resistance along the push pile. (It is frequently assumed that the shaft resistance in pull is significantly smaller in pull as opposed to in push. This contention is based on very dubious data, however. For a discussion on this subject, see Fellenius, 2002).

The uppermost diagram shows the predictions of total capacity as vertical bars, in ascending magnitude. Next to each total capacity "bar" is shown the predictor's submitted pull capacity. Below is shown the distributions of "shaft" and "toe" capacities organized in ascending magnitude. Therefore, a specific predictor's shaft capacity "bar" will not necessarily have the same sequence position as the predictor's toe capacity "bar".

The bulk of the predictions indicate a mean total capacity of about 1,000 KN with an approximately even split between shaft and toe resistances. This is at the low range of capacity values calculated from the before-the-event CPT soundings presented in the foregoing (Fig. 8).

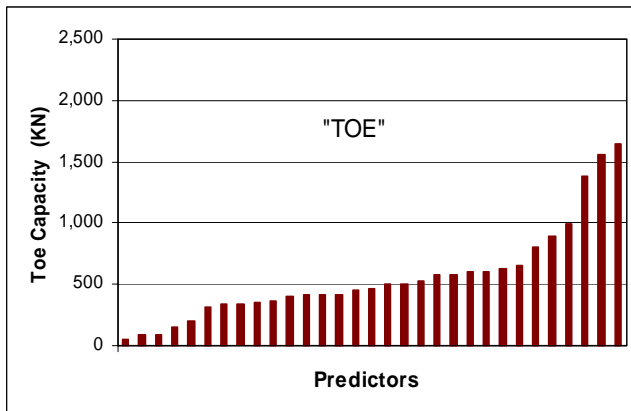
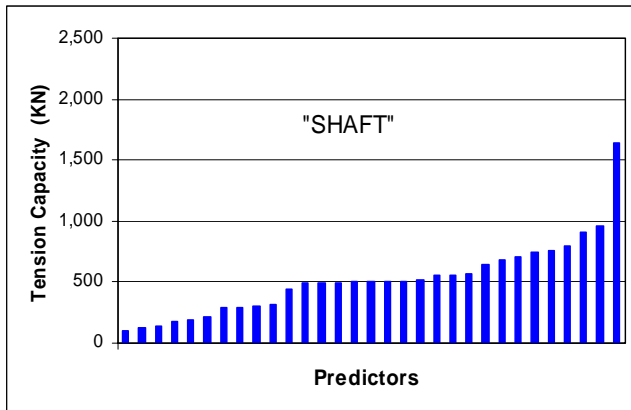
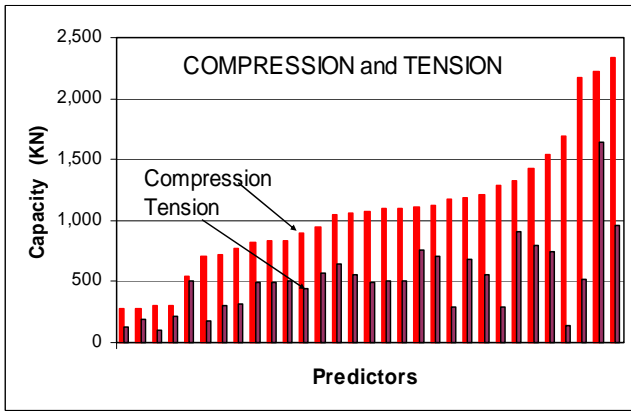


Fig. 11 Compilation of predicted capacities (Total, Shaft, and Toe)

A frequency chart of the predictions is presented in Fig. 12 showing the percentage of predictions within ranges of 400 KN. The diagram indicates that almost half of the predictions lie within the range of 800 KN through 1,200 KN. That is, half the predictors appear to agree rather closely about what the static loading test would show the pile capacity to be.

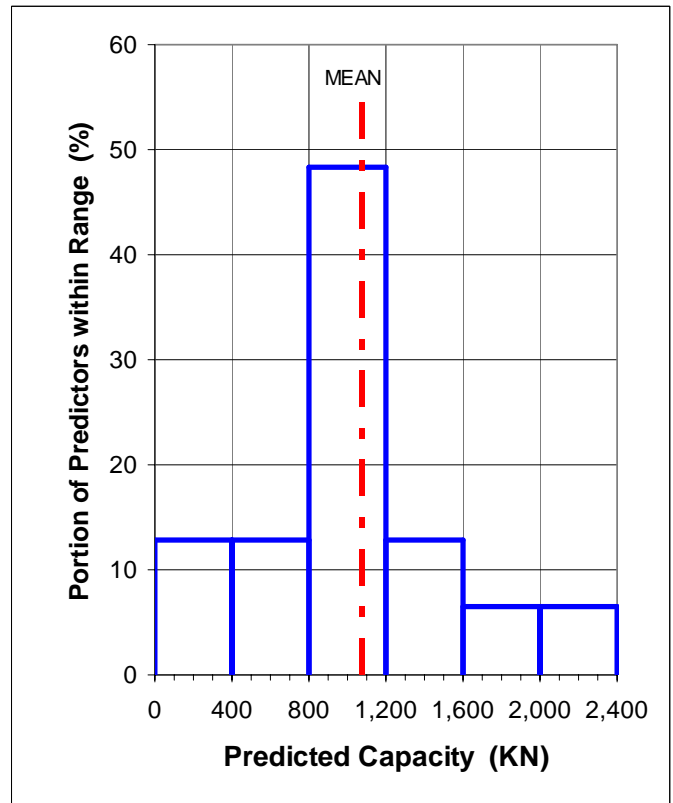


Fig. 12 Distribution of capacity predictions

### THE RESULTS OF THE STATIC LOADING TEST

Some time into the static loading test, it was noticed that the oversized steel plate placed on the pile head, to which the dial gages were attached, was becoming dished, resulting in inaccurate movement measurements. The pile was unloaded, a thicker plate was added, and the test started anew. The records of the loading and unloading were not kept. Then, an additional quandary arose: The load values determined from the jack pressure readings and from the independent load cell readings differed by a factor of 2 from one another. Obviously, one of the two calibrations had mistakenly noted loads in kips despite the loads being in tons. Or, conversely, noted tons despite the loads being in kips. After some discussion, it was agreed that the gage indicating the higher values gave the correct loads and the test proceeded. When the indicated load was 1,250 KN (281 kips), it was noticed that the hydraulic jack expanded without being associated with a pressure increase in the jack or load reading on the load cell. When the pumping continued, one corner of the reaction platform lifted and the test had to be abandoned for safety reasons. The dead weight on

the platform was made up of 16 about 25 ft long pieces of 24" concrete pile and it was determined to be about 1,100 kN (240 kips) and the platform itself was estimated to provide an additional 100 kN of weight. Fig. 13 shows a photo of the set-up. Moreover, it was considered unlikely that the center of gravity of the weights and platform would be very much offset from the pile location. Therefore, those present were reaffirmed in their opinion that the registered load of 1,250 kN was probably correct.



Fig. 13 Arrangement of static loading test  
(Photo courtesy of Prof. J. Long)

A strain gage had been cast into the pile near the pile toe. At the 1,250 kN maximum load, the measured strain was stated to correspond to an increase of load at the pile toe of approximately 50 kN (10 kips). The value does not include the residual (locked-in) toe load present immediately before the start of the loading test, and the small toe resistance is a sign of that the capacity of the pile had not been mobilized when the test was abandoned.

The load movement curve up to the load when the test was abandoned is presented in Fig. 14. No data are available on the initial loading and unloading or on the final unloading of the pile. The load-movement curve is extrapolated with three dashed alternative curves. The upper and lower of the alternative curves are plausible behavior with the lower being for a pile with small toe resistance and the upper curve from a pile developing significant toe resistance. The middle curve is a curve suggested by Goble (2002) and the "X" indicates the offset limit load (Davisson Limit) for that curve.

The "Elastic Line" shown in Fig. 14 is the load-movement curve for the pile functioning as a column standing on an unyielding surface. At a load of 1,250 kN, the column shortening is calculated

to 14.0 mm. The movement of the pile head measured by the dial gages at the 1,250 kN load was 5.5 mm, which is too small to be true for an initial loading sequence. A pile with little toe resistance and uniformly distributed shaft resistance would show a pile shortening that is exactly equal to half the column shortening, i.e., 7 mm. The movement necessary to generate this shaft resistance and would be between 1 mm to 2 mm. Mobilizing even a small toe resistance would result in adding another millimetre or two of pile shortening. In initial (virgin) loading, therefore, such a pile would experience a pile head movement close to or even beyond the elastic line at the "abandonment load".

Assuming that the values of applied load are true, then, the 5.5 mm movement value is only correct if the shaft resistance in the upper portion of the pile is large, if the pile is affected by substantial residual load, and if the portion of the maximum load reaching the pile does not exceed the residual toe load. As

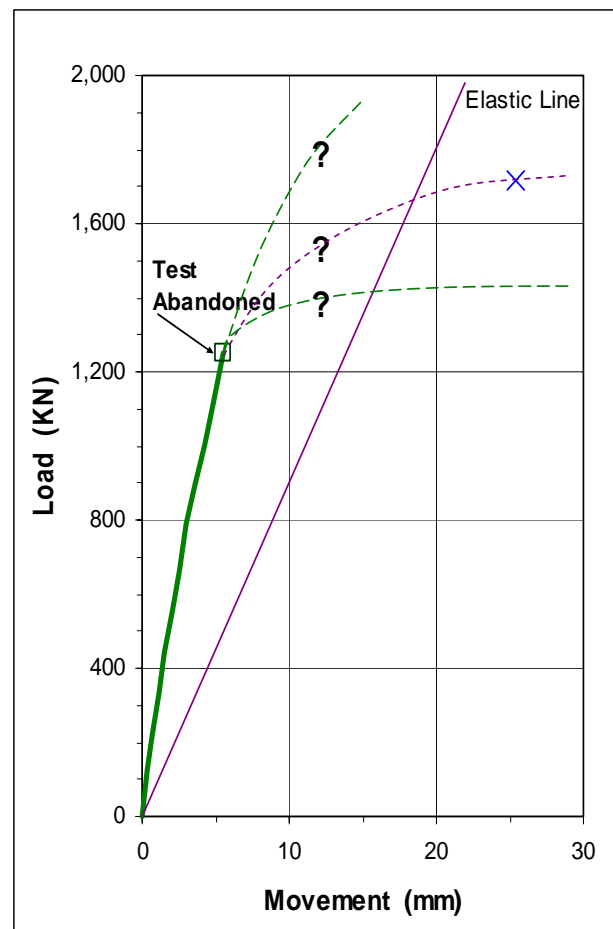


Fig. 14 Load-movement diagram from the static loading test

shown in Figs. 9 and 10, the dense, shallow layer provides a large shaft resistance, the first loading cycle will have built in a residual load in the pile, and the toe load measurements indicates that residual toe load was not exceeded. Therefore, the 5.5 mm movement at the maximum load is probably correct and consistent with that the load-movement curve is simply a reloading of the pile.

The outcome of the static loading test is a disappointment, of course. However, one lesson was learned: the prediction of the person charged with determining what reaction load to truck in for the static reaction is definitely more important than the prediction of all other participants in the event.

**THE RESULTS OF THE DRIVABILITY PREDICTIONS**

The demo pile as driven was a 50 ft (15.2 m) long, 12.75-inch (324 mm) diameter, closed-toe pipe pile with a 0.25 inch (6.35 mm) wall. The pile was ultimately driven to an embedment depth of 45 ft (13.7 m) using an APE D8-32 diesel hammer (rated energy 24 KJ —17.7 kip-ft). The helmet weight was 7.8 KN (1.75 kips), the cushion material was MC901, the cushion area was 458 cm<sup>2</sup> (71 in<sup>2</sup>), and the cushion thickness was 40 mm (2 in).

Prediction of the drivability can be made using one's long-term experience of how different types of piles respond to driving in a particular area with reference to usually employed hammers. Lacking that, the only way is to obtain some feel for what lies ahead is to perform a wave equation analysis, the GRL WEAP being the most widely used program. When the soil density varies with depth at the site, the static soil resistance distribution with depth must be established and be input to the program. Such input needs only to be relative, so using the SPT N-index distribution is quite suitable, provided one has confidence in that it correctly reflects the soil resistance encountered by the pile driving. The CPT soundings are thought to be more reliable in this regard. However, all CPT methods are calibrated to pile capacities established in a static loading test after set-up. Any numerical distribution calculated from CPT data therefore provides an overestimated distribution of the static resistance. That is, the actual static resistance encountered by the pile during the driving will be smaller, perhaps much smaller. This is because the soil resistance breaks down during the driving and the lost portion will return as set-up during the wait between the driving and the static loading test. The difficult questions to decide are how large a break-down would occur. However, the WEAP can also input the CPT data as relative resistance. Of course,

the analysis would not reflect that different soil layers could show different set-up ratios.

Fig. 15 shows calculated distributions of soil resistance (shaft and toe) obtained from the six CPT soundings using the Eslami-Fellenius method. The three after-the-event CPT soundings show a considerably larger resistance as opposed to the three before-the-event soundings.

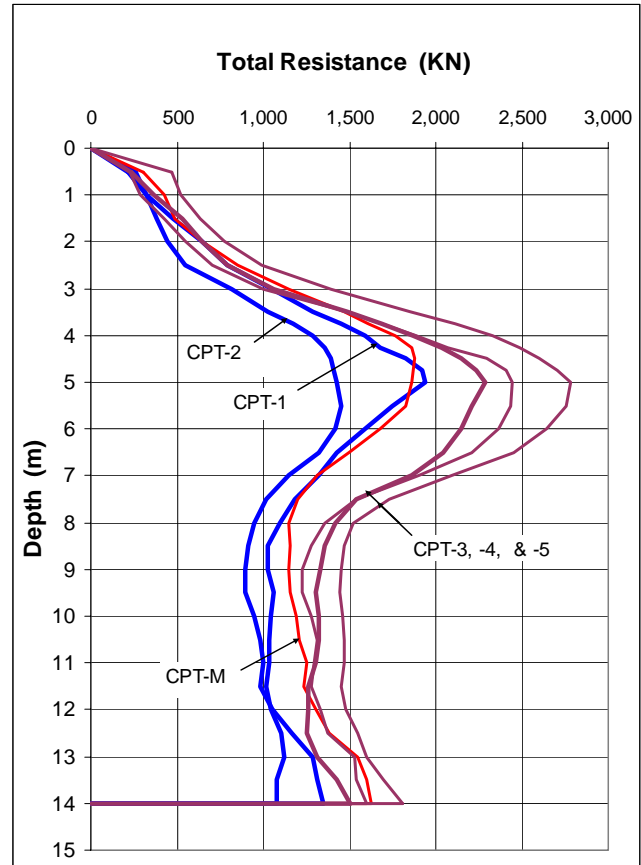


Fig. 15 Distribution of static resistance relative to driving

Fig. 16 shows two bearing graphs produced by GRL WEAP using “standard” input of quake and damping and input of shaft resistance distribution approximated from before-the-event soundings and toe resistance input as 50 % of shaft resistance. The analyses are made for “shallow” depth, i.e., in the middle of the dense layer at about 4.5 m and at full installation depth. It is obvious from the two curves that were the static resistances during the driving quantitatively about equal to that shown in Fig. 15, the APE D8-32 hammer would have difficulty driving the pile. (However, the hammer would work easily if the resistance was represented by either of the SPT borings).

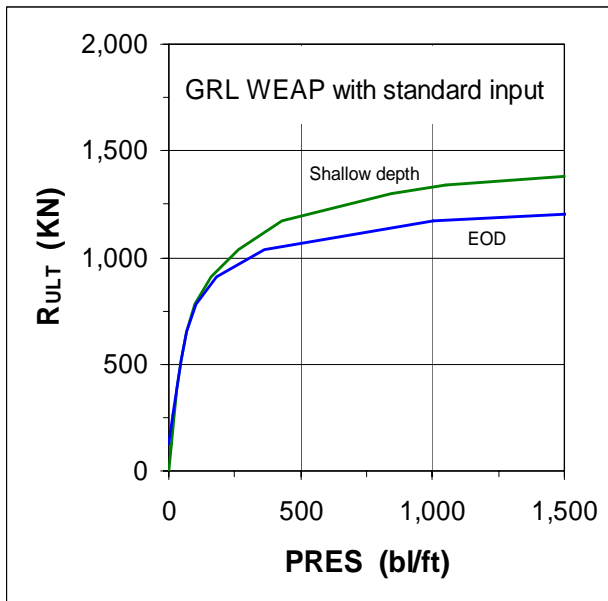


Fig. 16 WEAP Bearing Graphs

**THE OBSERVED PENETRATION RESISTANCE (BLOW COUNT)**

The recorded penetration resistances (PRES) for the three test piles are presented in Figs. 17A and 17B together with the diagrams submitted by the predictors. The two diagrams present the same data but use different scales for the penetration resistance (PRES). The prominent result is that all predictors expected a much smaller penetration resistance than that actually encountered. Only one predictor recognized the influence of the very dense shallow layer. Unfortunately, this predictor's values were shy toward the end of the driving. Therefore, because the drivability competition emphasized the termination driving, his prediction could not receive the recognition it deserved. The demo pile required more than 1,100 blows in the dense layer (depth of 4.2 m), a kind of PRES value for once properly characterized by the term "refusal". A blow count of this magnitude is not driving the pile, but more akin to creating a hole for the pile to go down in by crushing grains and compacting soil away from the pile. Also the PRES values of the push and pull piles are high in this layer, almost 200 blows/foot. Note, the practice in Florida is to consider 240 bl/0.3 m as "absolute refusal", and the selection of pile driving hammer is determined by the desire that it will operate within the range of 32 bl/0.3 m through 120 bl/0.3 m. A resistance beyond that range is considered "practical refusal", and is discouraged.

**RESULTS OF DYNAMIC MONITORING AND ANALYSIS**

The driving of each of the three piles was monitored with the Pile Driving Analyzer (PDA). The continuous records of the transferred energy (EMX) in the pile and the hammer blow rate (BPM—note the reversed scale) are presented in Fig. 18. (Because the resistance was so far beyond absolute refusal, the operator monitoring the driving of the demo pile ceased monitoring while the pile driving hammer was still trying to make the pile penetrate the dense shallow layer. Therefore, no records from the demo pile were obtained from below about 5 m depth). The blow rate is an inverse indication of the hammer rise and, therefore, of the kinetic energy at impact.

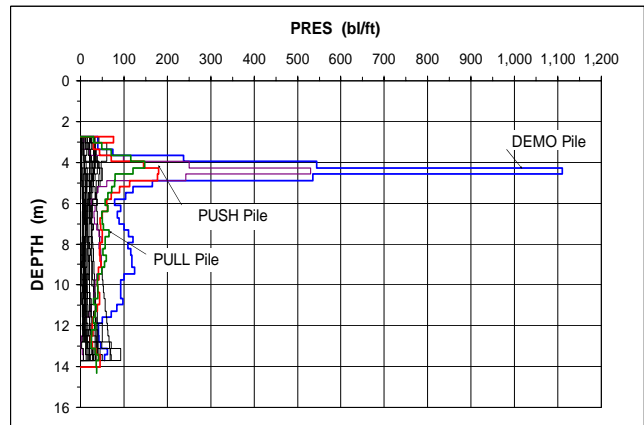


Fig. 17A Actual and predicted penetration resistance (PRES) diagrams

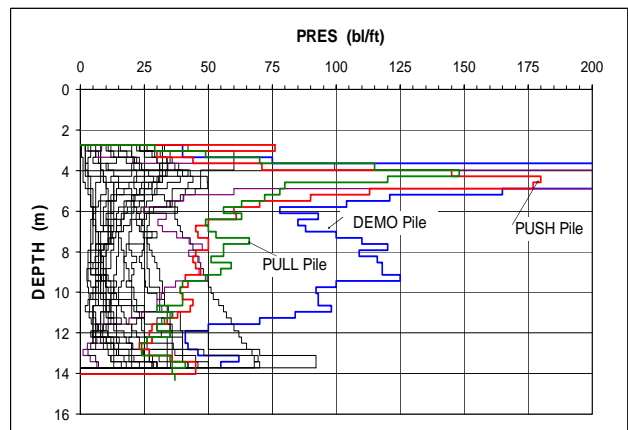


Fig. 17B Actual and predicted penetration resistance (PRES) diagrams

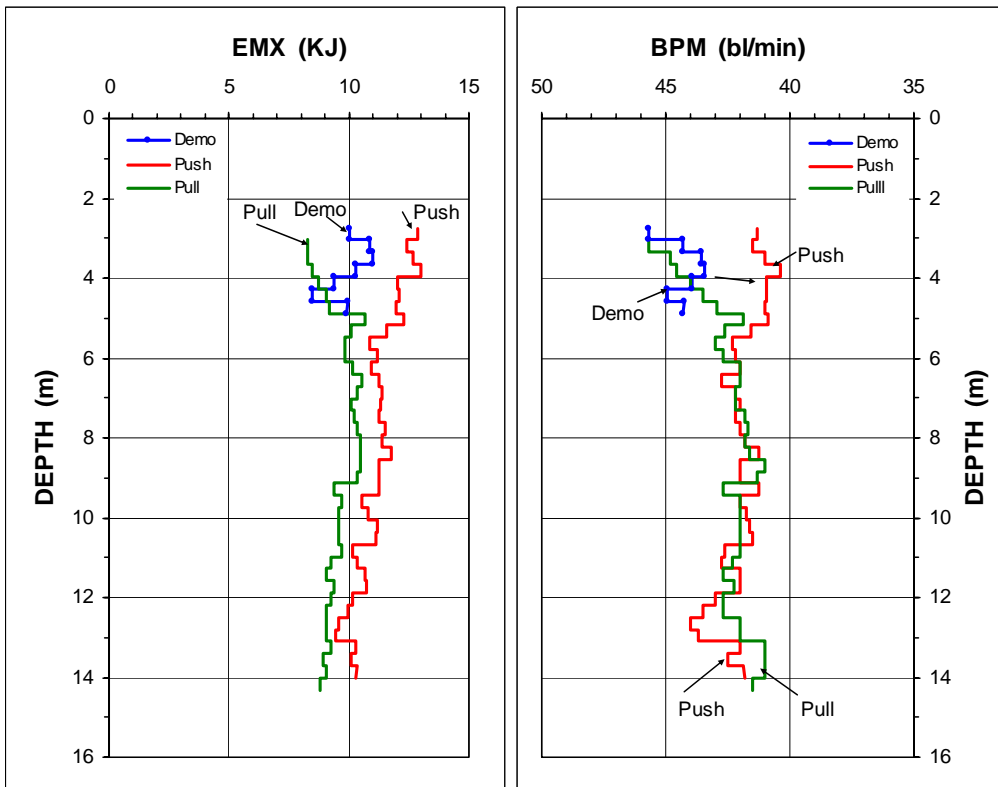


Fig. 18 Distribution of transferred energy (EMX) and blow rate (BPM)

The results show that the hammer energy when driving the piles in the dense shallow layer were appreciably larger for the push pile than for the pull pile and the demo pile — 12 KJ as opposed to about 8 KJ to 11 KJ. Initially, the EMX values indicated a smaller transferred energy for the pull pile as opposed to the demo pile. Below the dense, shallow layer, the values are about equal, but still smaller than those observed in driving the push pile. In contrast, the PRES diagram in Fig. 16 shows that the push and pull pile records were about the same and quite different from that of the demo pile. As so often is the case, the full answer is found when looking into the detailed results of the dynamic monitoring.

Blows from the driving in the dense, shallow layer and at end-of-driving (EOD) were selected for CAPWAP analysis and a WEAP analysis called CAPWEAP. The CAPWEAP analysis applies the actual hammer input for the analyzed blow to a range of static soil resistance with the distribution and soil parameters determined in the CAPWAP analysis. The CAPWEAP results are presented in Fig. 19 together with the two curves determined in the standard WEAP analysis (Fig. 16). The results indicate that in driving the push pile, the hammer performed in good agreement with standard values. However, in driving the demo pile and initially also the pull pile, the hammer did not perform as well.

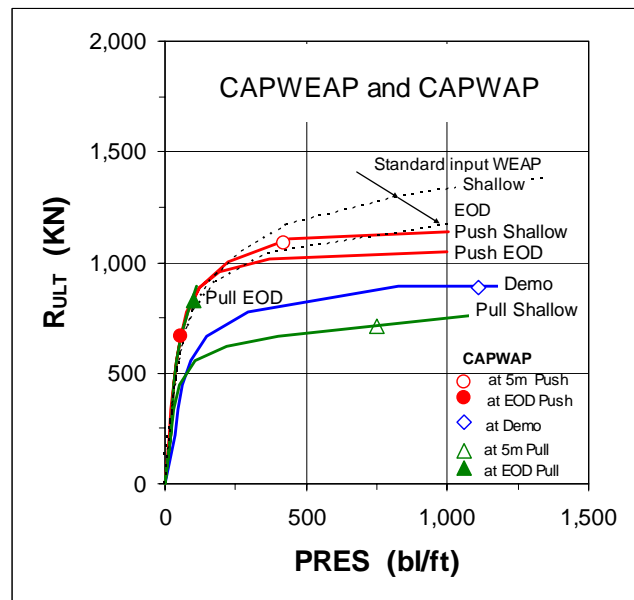


Fig. 19 Results of CAPWAP and CAPWEAP analysis

The Pile Driving Analyzer (PDA) records can be used to calculate a pile capacity value, called Case Method Estimate (CMES), for every blow given to the pile. The CMES value is a function of a damping factor that experienced operators usually can choose guided by wave traces and soil profile. Many CMES methods

are in use, the most commonly applied is called the R-max or RMX-method. It is often advisable to correlate the choice of damping factor and method to the results of a CAPWAP analysis of a blow or two, as the CAPWAP analysis is the more sophisticated analysis method. For the three piles, a good agreement with the CAPWAP results were obtained with the CMS RMX method and a damping factor of 0.7, i.e., RX7.

The CAPWAP-determined capacities at the end of the driving for the push and pull piles were 670 kN, and 710 kN, respectively. No restrrike tests were made. CAPWAP analysis of restrrike records would have been desirable as the analysis results are representative for capacity after set-up and suitable for comparison the results from a static loading test.

The PDA capacity records from the driving of the three piles are presented in Fig. 20 compiling the RX7 and CAPWAP values. For reference, the static resistance distribution (shaft and toe) obtained from the CPT soundings at the test site are also shown. Considering the large difference in penetration resistance (PRES) in the dense shallow layer and in the deeper layer, at first glance, it is surprising that the RX7 capacity values in the dense shallow layer only differ by a 100 kN to 200 kN. However, as indicated in the bearing graphs (Figs. 16 and 19) a resistance of about 800 kN will correlate to a PRES value of about 50 bl/0.3 m, and, as the graphs make clear, increasing the capacity by a small amount, about 200 kN, will result in a many times larger PRES value. In other words, the hammer operated very close to its maximum for the particular hammer-soil combination. When the hammer energy decreased, as in the case of the demo pile, the penetration resistance increased considerably.

The difference between the RX7 capacity values and the capacities calculated from the CPT soundings is a bit more challenging to explain. First, however, the much larger capacity values calculated from the after-the-event soundings may be due to the fact that the soundings reflect densification caused by the pile driving. CPT-3, placed 1.5 m from the demo pile, shows the largest capacity. CPT-5, placed 3.0 m away from the push pile shows smaller capacity distribution, but still larger than the distribution shown by CPT-4 placed 7.0 m away from the nearest pile. It is therefore, quite likely that had the cone tests been made before the piles were driven, they would have shown a capacity distribution similar to those shown by the before-the-event soundings. However, the after-the-event CPT soundings may well better represent the conditions for the static loading test as opposed to the before-the-event soundings that do not include effect of densification. It is therefore a pity

that available resources did not allow the piles to be restruck after the static loading test (with PDA monitoring and CAPWAP analysis, of course).

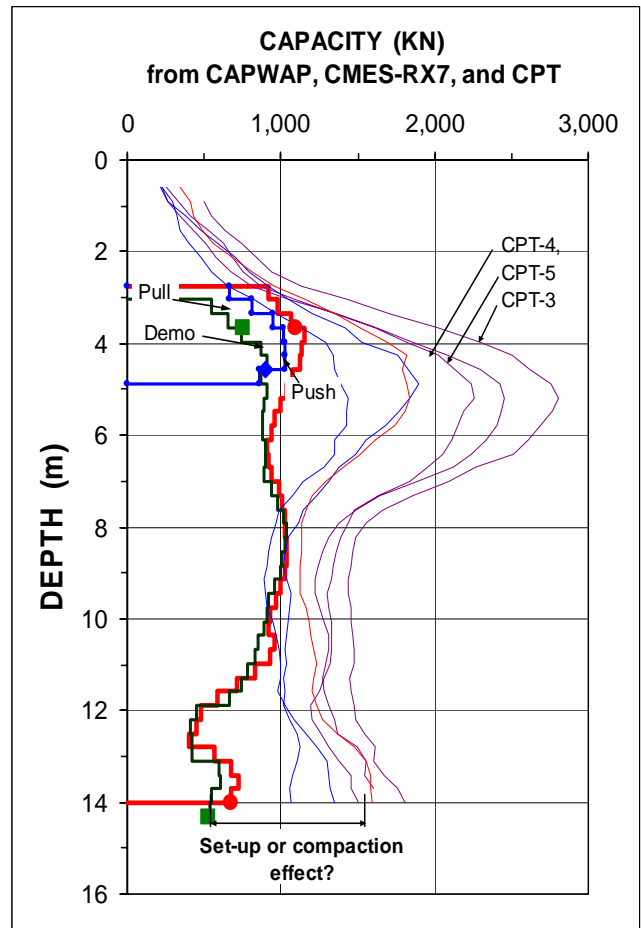


Fig. 20 Distribution of resistance (kN) to driving calculated by CMES RX7, CAPWAP, and CPTU

Note, the RX7 capacities and the EOD CAPWAP values are from the initial driving of the pile, whereas the CPT capacity values represent the long-term conditions. The CPT analyses suggest that the pile capacities would have increased considerably after set-up, indeed doubled or more. Although no “proof” exists that the CPT-calculated capacities are true, the suggested set-up increase is entirely in keeping with the local experience of set-up in sand, as, for example, indicated by McVay et al. (1999).

Finally, it should be noted that the CPT calculations indicate a thicker dense, shallow layer than suggested by the RX7 distribution. First, the CPT calculations combine the cone stress values within 8 pile diameters above the pile toe and 4 pile diameters below. When going from a dense soil and into a

looser soil, it may be preferable to shorten the distance above the pile toe to 4 diameters. This would have reduced the thickness of the high capacity zone by about 1 m when making capacity calculations from

CPT data. In addition, one must consider that the small diameter of the cone does not feel any effect from the softer layers until the cone is within about 0.2 m above the softer layer, whereas the pile feels that effect more than 1 m higher up.

The CAPWAP analysis also produced a load-movement diagram, which is presented in Fig. 21. The diagram also includes the load-movement curve from the static loading test placed at the unloading portion of the CAPWAP curve. Although the pile capacity at the time of the static loading test was arguably larger than the static resistance present at the dynamic test, the larger stiffness response represented by the slope of the curve of the static test, is only acceptable in view of that the test was a reloading cycle. The curve is plotted at the CAPWAP unloading portion to facilitate the comparison between an unloading and reloading curve.

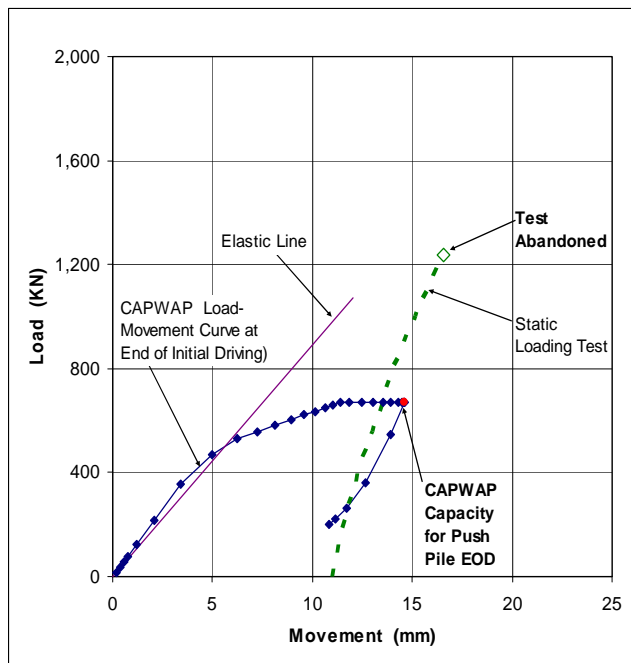


Fig. 21 CAPWAP simulation of EOD push pile records and Load-movement curve from the static loading test

## CONCLUSIONS

The results of the static loading test show that the planners of the test did not appreciate the potential of Murphy's Law and its effects on the event. In the case of the pile prediction event, almost everything that could go wrong did go wrong. The design of the static loading test apparently relied on calculations or estimates made using only the SPT data. A review of the other soils investigation data would have suggested the advisability of a larger reaction system so that the test load could have reached the ultimate resistance of the pile. Problems with the instrumentation prevented assured measurement of the loads and displacements of the push pile. The pull test could not be completed due to a premature failure of the tension connection to the pile. The test pile for the demonstration of pile driving ("demo pile") reached, and far surpassed, "Absolute refusal" penetration resistance at a depth of only 4 m, due in part to poor operation of the pile hammer.

Too much uncertainty rests with the data from the static loading test and this fact plus the poor performance of the hammer at the demo test removed the value of the event for its intended purpose as a prediction event. The good CPT and the dynamic monitoring data still provided good food for thought and, in spite of the problems, there is much to be learned from the event.

In a real world project, when directly applicable experience needed to answer the questions is unavailable, testing is necessary before design questions can be answered, indeed, sometimes even before the questions can be phrased. Projects involving driven piles need, in addition to site exploration, which should include both borings (SPT) and cone penetrometer tests (CPTU), a pile driving test which should be combined with dynamic monitoring of the driving and analysis. It is important that a restrike test with dynamic monitoring is performed some time after the initial driving.

The static loading test is a valuable design tool, but costly, and usually only warranted when the questions involve long-term behavior of the piles, settlement concerns, and other more involved situations, in which case the test pile(s) should be instrumented so that the distribution of load and resistance, as well as of residual load, can be established.

## **ACKNOWLEDGEMENTS**

The use of the site was provided by Giken Company, Orlando, Florida. The soil borings were performed by Nodarse and Associates, Winterpark, Florida. An initial CPTU was supplied by Georgia Institute of Technology. The CPT soundings were performed by Andaman & Associates, Inc., Tampa, Florida. The test piles were supplied by Manual Pipe Company of Lilburn, Georgia. The hydraulic jacks used for the static loading tests were furnished by Ellis and Associates, Jacksonville, Florida. The pile driving and static testing was carried out by Ed Waters and Sons Contracting Company, Jacksonville, Florida. The dynamic analyses were performed by GRL Engineers, Orlando, Florida. The authors wish to express appreciation to Dr. George G. Goble for his many valuable comments on the analysis.

## **REFERENCES**

CANADIAN FOUNDATION ENGINEERING MANUAL, CFEM, 1992. Third Edition. Canadian Geotechnical Society, Biotech Publishers, Vancouver, 512 p.

ESLAMI, A., 1996. Bearing capacity of piles from cone penetrometer test data. Ph. D. Thesis, University of Ottawa, Department of Civil Engineering, 516 p.

ESLAMI, A. and FELLENIUS, B.H., 1997. Pile capacity by direct CPT and CPTu methods applied to 102 case histories. Canadian Geotechnical Journal, Vol. 34, No. 6, pp. 886 - 904

FELLENIUS, B.H. and GOUDREAU, P.A., 1998. UniPile Users Manual, UniSoft Ltd., Ottawa, 45 p

FELLENIUS, B.H. and ESLAMI, A., 2000. Soil profile interpreted from CPTu data. Proceedings of Year 2000 Geotechnics Conference, Southeast Asian Geotechnical Society, Asian Institute of Technology, Bangkok, Thailand, November 27 - 30, 2000, Vol. 1, pp. 163 - 171.

FELLENIUS, B.H., INFANTE, J-A., 2002. UniCone Version 1 Users Manual, UniSoft Ltd., Calgary, 35p.

FELLENIUS, B.H., 2002. Axial Loading Tests on Bored Piles and Pile Groups. Discussion. ASCE Journal of Geotechnical Engineering, Vol. 128, No. 11, pp. 283 - 284.

GOBLE, G.G., 2002. PDCA sponsors pile demonstration. Piledrivers.org, Spring 2002. Vol. 3, No. 2, pp. 27 - 28.

McVAY, MR., SCHMERTMANN, J., TOWNSEND, F, and BULLOCK, P. (1999). Pile freeze, a field and laboratory study. Final Report, Florida Department of Transportation, Research Center, Contract No. B-7967, 1,314 p.

MEYERHOF, G. G., 1976. Bearing capacity and settlement of pile foundations. The Eleventh Terzaghi Lecture, November 5, 1975. American Society of Civil Engineers, ASCE, Journal of Geotechnical Engineering, Vol. 102, GT3, pp. 195 - 228.